

Intensity Dynamics in Semiconductor Laser Arrays

Matthew O. Williams¹, Mingming Feng², J. Nathan Kutz¹,
Kevin L. Silverman³, Richard P. Mirin³, and Steven T. Cundiff²

¹Department of Applied Mathematics, University of Washington, Seattle, WA 98195

²JILA, University of Colorado and National Institute of Standards and Technology, Boulder, CO 80309

³National Institute of Standards and Technology, Boulder, CO 80305

kutz@amath.washington.edu

Abstract: The dynamics of a five-emitter semiconductor laser array is studied theoretically with steady-state, oscillatory, and chaotic behaviors achieved. This provides a design tool for achieving oscillations whose frequency is related to injection current.

© 2009 Optical Society of America

OCIS codes: (140.5960) Semiconductor lasers, (230.7370) Waveguides

1. Introduction

Semiconductor laser arrays are capable of producing high output powers if the array can be phase locked in an in-phase fashion. However, experimental and numerical simulation have shown that, even for two-emitter arrays, the undesirable stable out-of-phase state is favored over the in-phase state [1, 2]. Additionally, once the coupling strength between adjacent emitters exceeds a critical level, the array begins to operate in an unstable manner. Rahman, Winful, and others have shown there are diverse intensity dynamics for one-, two-, and three-emitter arrays [2–5]. The behaviors observed for those arrays include chaos and sustained self-stable oscillations. In a similar approach to Rahman and Winful, the intensity dynamics of a five-emitter array are examined. In addition to the larger number of emitters, an injection current that decreases with successive emitters is included. The oscillatory dynamics of this system are of particular interest. In that regime, such an array has the potential for application as an all-optical GHz oscillator. Ultimately, the analysis of this larger array has shown that it is capable of exhibiting the same types of stable out-of-phase, oscillatory, and chaotic behaviors exhibited by the smaller arrays, and that the numerical model is able to accurately capture the results of experiment for a five emitter quantum-dot laser.

2. Governing Equations

The governing equations for this array are derived from Maxwell's equations for the field and the diffusion equation for the carrier density. The model itself includes several important physical phenomena such as guided mode propagation, evanescent field coupling between waveguides, spatial diffraction, stimulated emission and absorption, and carrier antiguiding. In principle, this is a problem with three spatial dimensions, but to reduce the dimensionality of the problem, a TE mode, the slowly varying envelope approximation, and the effective index method are assumed. Additionally, the loss due to transmission through the facets are distributed over time, and the carrier density is assumed to be uniform in the direction of propagation [2]. These assumptions reduce the problem to the pair of coupled differential equations (1).

The PDE system depends upon a large number of physical quantities, but their impact can be combined into a reduced number of nondimensional quantities as follows: $U = (\eta_e^2 g \tau_s / 2c \eta_a)^{1/2} \psi$, $V = \frac{1}{2} g \tau_p (N - N_{th})$, $p(x) = \frac{1}{2} g \tau_p [j(x) \tau_s - N_{th}]$, $T = \tau_s / \tau_p$, $g = \Gamma a c \eta_a / \eta_e^2$, $1/\tau_p = (c/\eta_e)[(\eta_c/\eta_e)(1-\Gamma)\alpha_c + (2/L) \ln(1/r)]$, $N_{th} = N_0 + 1/g\tau_p$, $L_p = (c\tau_p/2\eta_e^2 k_0)^{1/2}$, $C = \Gamma c k_0 \eta_a \tau_p / \eta_e^2$, and $\tau = t/\tau_p$. In these substitutions, η_a , η_c , and η_e are the indexes of refraction of the active and cladding layers as well as the effective index. Γ is the transverse confinement factor, L is the length of the cavity, r is the reflection coefficient at the facets, N_0 is the carrier density for transparency, k_0 is the wavenumber, τ_p is the lifetime of a photon, and a is the gain coefficient. The system of equations becomes

$$\frac{\partial U}{\partial \tau} = iC \Delta \eta_{\text{eff}} U + (1 - iR)UV + iL_p^2 \frac{\partial^2 U}{\partial x^2} \quad (1a)$$

$$T \frac{\partial V}{\partial \tau} = p(x) - V - (1 + 2V)|U|^2 + L_e^2 \frac{\partial^2 V}{\partial x^2}. \quad (1b)$$

In (1), U is related to electric field envelop and V is related to the charge carrier density relative to the threshold value. $p(x)$ is the injection current relative to the threshold level and, in this case, is not of constant value in each waveguide. C

and Δn_{eff} model the strength the lateral guiding due to changes in the effective index. R is the antiguiding parameter, which models changes in the index of refraction due to the presence of charge carriers. Lastly, T represents the characteristic timescale of the carrier dynamics relative to the timescale of the optical field dynamics. These equations were solved numerically using Crank-Nicolson with a time splitting method to handle the carrier dynamics and also using transparent boundary conditions, the peak intensity in each emitter is used as a measure of the output power of an emitter [2, 6].

3. Results

Numerical experimentation with this PDE model were able to reproduce all of the dynamics exhibited by smaller systems. Among those behaviors are the stable out-of-phase state, sustained oscillations, and chaos. Numerical results for the oscillatory regime are shown in Fig. 1(a). In this figure, the first waveguide is shown in solid black, the second in dashed black, the third in solid gray, and so on. As expected from the analysis of smaller arrays, one parameter that determines the response of the system is the separation of the emitters. Larger separations imply weaker coupling, resulting in the stable out-of-phase behavior. Intermediate values produce oscillations, and small values of waveguide separation produce chaos.

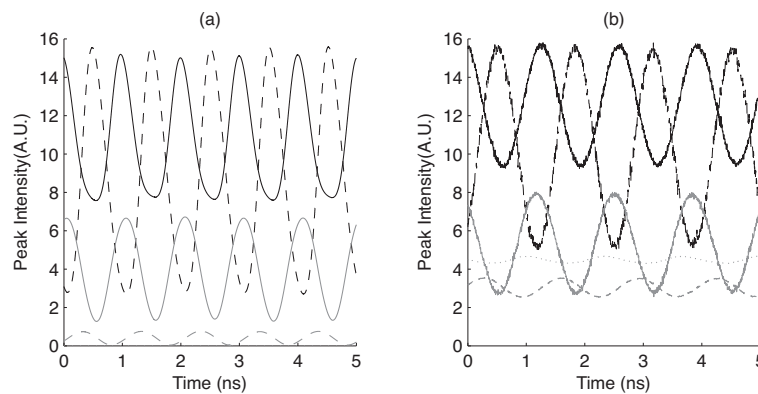


Fig. 1: Plot of peak intensity vs time for the numerical simulation and experimental results, shown in (a) and (b) respectively, while operating in the oscillatory regime. There is good agreement between experiment and numerical results particularly with respect to the amplitude and frequency of oscillation.

The injection of a nonuniform current also has an impact on the dynamics of the system. With uniform injection current, the output power varies between the emitters. In particular, the center emitter or center pair of emitters will output higher powers than the outer emitters. This is due to the outer emitters having no adjacent waveguides with which they can couple. The obvious behavior of a nonuniform injection current is to break that symmetry.

This impact of the nonuniform injection current persists in both the oscillatory and chaotic regime. Example results from the oscillatory regime, shown numerically in Fig. 1(a) and experimentally in Fig. 1(b), reflect the same general trend in the stable case, higher injection current produces higher output power. However, due to the increased level of coupling, the difference in average output power is not as pronounced as in the stable case as it is easier for emitters to couple energy between themselves. This also influences the amplitude of oscillation. As shown in smaller arrays, the center waveguides typically exhibit the largest oscillations when the injection current is uniform [2]. Again, the uneven current is able to partially counteract and create the largest oscillation in another element of the array. Additionally, it is possible to induce phase shifts other than the nearly π phase shift in the uniform case by changing the slope of the current. Therefore, alterations in the slope of the injection current can produce additional dynamics that are not seen in the uniform case.

However, the physical parameter of particular experimental interest is the oscillation frequency of the intensity. For some configurations, this oscillates in the GHz range allowing the system to be used as an all-optical GHz oscillator. The only parameter which can be readily altered experimentally is the injection current. To test the accuracy of this approach, the frequency of oscillation is compared to experimental results from a five-emitter AlGaAs quantum-dot laser array. In this comparison, there is good quantitative agreement between the experiment and the theory. In particular, the response of this system to changes in injection current shown in Fig 2. Overall, the fundamental frequency of oscillation as well as the higher harmonics match well with the experimental data. The fundamental

JTUB14.pdf

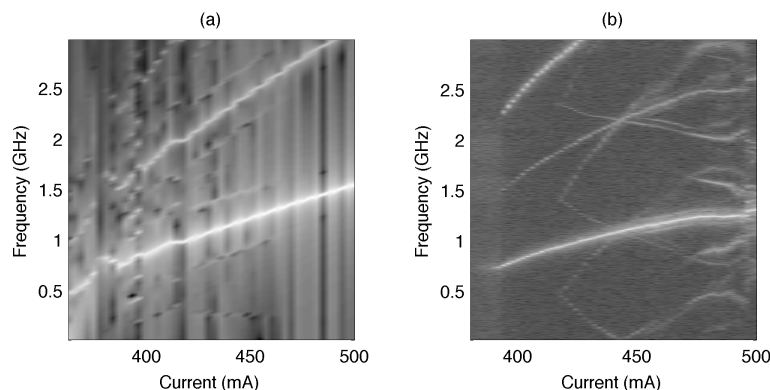


Fig. 2: A plot of the frequency components of the output power of an array operating in the oscillatory regime. Numerical results are shown in (a) and experimental results shown in (b). The output power is in decibels and lighter colors represent higher powers. Note that most of the output is defined by a fundamental frequency of oscillation, but there are also higher harmonics and fine structure evident in both experimental and numerical results.

frequency of the numerical simulation increases from 0.75 GHz to 1.5 GHz while in experimental results the increase is from 0.75 GHz to 1.25 GHz. Also evident in both cases is a second and third harmonic. In addition, there is fine structure between the harmonics exhibited in both theory and experiment. These results are dependent upon a large number of physical parameters including injection current and waveguide geometry.

4. Conclusions

Ultimately, the different dynamical responses of the smaller one-, two-, and three-emitter arrays were reproduced on a five-emitter array. These behaviors include the stable out-of-phase, oscillatory, and chaotic regimes. The addition of an nonuniform injection current allows the observation of additional dynamical responses and methods for altering the average intensity and magnitude of oscillations of the resulting dynamics.

Particular experimental interest is in the regime where the array is producing stable oscillatory output. There, the fundamental frequency of oscillation is sensitive to changes in the injection current. For physically realistic parameter values, we have shown this model can be used to model the response of laser arrays acting as GHz oscillators. The model accurately captures the frequency of oscillations as well as the that of the higher harmonics, and it also achieves the fine structure similar to that observed in experiment. Overall, this relatively simple model of a semiconductor laser array gives good quantitative agreement with experimental results and can be used as a design tool for arrays operating in this regime.

References

- [1] B. Botez and G. Peterson, "Modes of phase-locked diode-laser arrays of closely spaced antiguides," *Electronics Letters* **24**, 1042–1044 (1988).
- [2] L. Rahman and H. G. Winful, "Nonlinear dynamics of semiconductor laser arrays: a mean field model," *IEEE Journal of Quantum Electronics* **30**, 1405–1416 (1994).
- [3] S. Wang and H. Winful, "Dynamics of phase-locked semiconductor laser arrays," *Appl. Phys. Lett* **52**, 1774–1776 (1988).
- [4] L. Rahman and H. Winful, "Improved coupled mode theory for the dynamics of semiconductor laser arrays," *Optics Letters* **18**, 128–130 (1993).
- [5] S.-S. Wang and H. G. Winful, "Propagation model for the dynamics of gain-guided semiconductor laser arrays," *J. Appl. Phys* **73**, 462–464 (1993).
- [6] G. R. Hadley, "Transparent boundary condition for beam propagation," *Optics Letters* **16**, 624–626 (1991).